Journal of Materials Processing Tech. 254 (2018) 114–123

Contents lists available at ScienceDirect

Journal of Materials Processing Tech.

journal homepage: www.elsevier.com/locate/jmatprotec

Enhancement of fatigue resistance for 316L welds produced by magnetic field assisted laser-MIG hybrid welding

Rong Chen[a], Ping Jiang[a,*], Xinyu Shao[a], Gaoyang Mi[b], Chunming Wang[b]

[a] The State Key Laboratory of Digital Manufacturing Equipment and Technology, School of Mechanical Science and Engineering, Huazhong University of Science & Technology, 430074 Wuhan, PR China

[b] School of Materials Science and Engineering, Huazhong University of Science & Technology, 430074 Wuhan, PR China

ARTICLE INFO

Keywords:
Crack propagation
Crystallography texture
Electron backscattering diffraction
Magnetic field
Laser-MIG hybrid welding

ABSTRACT

Crack growth rate (CGR) in air for welds produced by 24 mT magnetic field assisted laser-MIG hybrid welding was decreased by 33%. CGR in 3.5% NaCl solution for welds produced by 16 mT magnetic field assisted welding was reduced by 20%. Texture variation in welds was investigated through electron backscattered diffraction (EBSD). External magnetic field lowered thermal gradient and changed orientations of maximum thermal gradient (∇T_{max}), resulting in weaker texture intensity and less ferrite. Reduced intensity of {100} planes and ⟨100⟩ orientations improved resistance to cyclic plastic deformation. Reduced ferrite increased the volume of strain-induced martensite at crack tip, improving fatigue cracking resistance.

1. Introduction

Austenitic stainless steels combine high corrosion resistance and good mechanical properties, however, its welds show poor resistance to fatigue crack. Wu et al. (2016) showed that conventional welding process with extremely high heat input and quick cooling rate, often induced high temperature gradients and undesirable microstructures. Thus, it is indispensable to propose an innovative and effective welding method to improve fatigue resistance of welded joints.

Electromagnetic processing of materials (EPM) has attracted significant attention in metal processing industry. Chen et al. (2011) showed that external magnetic field significantly improved weld morphology and refined grains. Shoichi et al. (2013) confirmed that external magnetic field reduced weld defects and improved service behavior of the joints. Despite the numerous papers that deal with the weld shape variation and defect inhibition, information concerning the effect of magnetic field on phase transformation and texture variations needs to be more detailed.

There are some reports on effects of phases on fatigue resistance for austenitic stainless steel. Wang et al. (2016a, 2016b) proposed that higher density of slip bands and dislocations in γ-austenite prevented crack initiation and propagation for duplex stainless steel. Byung et al. (2000) reported that strain incompatibility between δ-ferrite and matrix promoted crack initiation, therefore increased the crack growth rate. Dong et al. (2017) exhibited that δ ferrite phase had a higher Cr content than γ austenite, leading to the formation of Cr_2O_3 film at crack tip when a propagating crack intersected with the δ ferrite. However, this phenomenon appeared in 308L rather than 316 due to the larger volume of ferrite in 308L. Besides, Abe and Watanabe (2012) reported that δ-ferrite in island-shaped morphology was of high resistance against stress corrosion cracking in high temperature water. Therefore, it is valuable to discuss effect of phases on the fatigue cracking resistance.

Arafin and Szpunar (2009) proved that crystallographic texture was crucial to the resistance of welded joint against fatigue cracking. King et al. (2008) showed that grain boundaries adjacent to low {hkl} index plane were resistive against intergranular stress corrosion cracking in austenitic stainless steel. Lavigne et al. (2014) discussed the influence of crystallographic texture on intergranular stress corrosion crack paths. Eghlimi et al. (2015a,b,c) showed that in austenitic stainless steel welded zone, columnar grains often formed with ⟨100⟩ orientations perpendicular to the fusion line. By finding effect of ⟨100⟩ texture on fatigue propagation, fatigue properties of 316L welds can be well understood and consequently optimized.

* Corresponding author.
E-mail address: jiangping@hust.edu.cn (P. Jiang).

https://doi.org/10.1016/j.jmatprotec.2017.11.030
Received 3 July 2017; Received in revised form 16 November 2017; Accepted 17 November 2017
0924-0136/ © 2017 Published by Elsevier B.V.

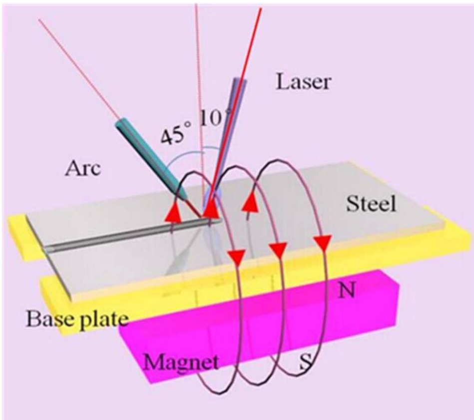

Fig. 1. Schematic of experimental set up.

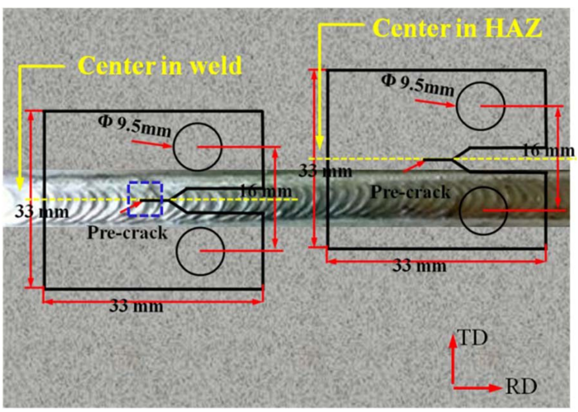

Fig. 2. Dimensions of compact tension specimen and schematically illustration of sampling locations.

In this paper, external magnetic field was applied during laser-MIG hybrid welding 316L stainless steel. Fatigue crack growth rates (CGRs) of 316L welds were measured and compared. Effect of external magnetic field on texture variation and its impact on CGR were discussed. Besides, the authors' previous work Chen et al. (2017) revealed that stirring effects brought by magnetic field decreased the δ-ferrite. Effects of decreased δ-ferrite on fatigue crack propagation rate were discussed in this paper.

2. Experimental details

2.1. Material and welding procedure

SUS 316L plates of 6 mm thickness were used in this study. Austenitic stainless steel ER 316L filler wire with 1.2 mm in diameter was employed for the bead-on-plate weld. Schematic of the setup was shown in Fig. 1. Details regarding magnetic-laser-MIG welding equipment and parameters were reported in the authors' previous publication Chen et al. (2017). External magnetic field intensity was set from 0 mT 32 mT. Welding direction was parallel to the rolling direction (RD).

2.2. EBSD characterization

EBSD analysis was carried out using FEI Sirion 200, an ultra-high resolution Schottky field emission scanning electron microscope. Working distance was adjusted to 17 mm with a 70° tilt angle under a high-current electron beam. Accelerating voltage of the electron gun was set as 20 kV. Kikuchi pseudo-bands patterns were collected, indexed and analyzed via OIM data collection software. Two parts of the EBSD characterizations were conducted in this study.

After welding, cross-sectional samples were prepared to analyze texture distribution in column zone of the welded joint. Then the specimens were ground, mechanically and electrochemically polished to remove the residual stress on surface. EBSD step sizes were 1.5 μm to characterize grain orientations in welded zones and heat affected zones.

After fatigue tests, cracked samples were cut and prepared at the blue rectangle region as showed in Fig. 2. Crack tip was included in the specimen. EBSD scans were conducted on horizontal plane of the specimen parallel to the RD-TD plane. In order to capture the accurate phase constituents at crack tips, an extremely subtle step size of 0.1 μm was chosen.

2.3. Fatigue crack propagation rate evaluation

After crowns of the welds were removed, welded joints were machined into standard compact tension (CT) according to ASTM (2005). Specimens were utilized with thickness of 5 mm and 33 mm in width. Detailed dimensions of CT specimens and illustration of sampling locations were schematically displayed in Fig. 2. They were pre-cracked in laboratory air at near-threshold stress intensities to generate a sharp crack with minimal residual stress until a/W = 0.43, in which $\boldsymbol{a}$ represented the crack length and $\boldsymbol{W}$ was effective length of the CT specimen. During fatigue crack growth rate tests, variation of **a/W** was defined as crack length increment which was real time monitored using a direct current potential drop (DCPD) technique. Evaluation procedure of DCPD was conducted by comparing the measured values of electrical potential variation with those calculated from an analytical method where the crack was modeled. Crack growth rate was directly reflected by the **a/W ∼ T** curve. Then the tests on fatigue crack growth rate were firstly performed in air at constant K_{max} = 25 MPa√m under ratio R = 0.3 (R = K_{min}/K_{max}), f = 0.1 and 1 Hz, then the environment was changed into 3.5% NaCl solution. During testing in 3.5% NaCl solution, parameters were kept the same with those in air.

3. Results

3.1. Fatigue crack growth rate

CGRs in WZs via different magnetic fields were listed in Fig. 3. Decrease of the frequency from 1 Hz to 0.1 Hz reduced the CGRs. Average CGR of 7×10^{-6} mm/s was observed at K_{max} = 25 MPa√m, R = 0.3, f = 0.1 Hz for specimens welded in the absence of an external magnetic field (WZ–0 mT) in air condition. Under the same test condition, lower CGRs were observed in specimens welded in the presence of external magnetic field. It was improved by 33% for specimens welded under 24 mT magnetic field (WZ–24 mT). Higher CGRs were observed for all the WZs as the environment changed from air to 3.5% NaCl solution. Average CGR of 1.5×10^{-5} mm/s was observed at K_{max} = 25 MPa√m, R = 0.3, 0.1 Hz for WZ-0 mT specimens in 3.5% NaCl solution. Under the same test condition, lower CGRs were observed in specimens welded in presence of external magnetic field, especially, improved by 20% for WZ-16 mT. As summarized in Fig. 3(f), in both air and 3.5% NaCl solution, lower CGRs were obtained for WZs produced by magnetic field assisted laser-MIG welding.

Results of CGR for BM and HAZ under different magnetic fields were listed in Fig. 4. It was obvious that CGRs were different at each zone of welded joint. CGR in BM was higher than that in HAZ. CGRs in HAZ

Download English Version:

https://daneshyari.com/en/article/7176520

Download Persian Version:

https://daneshyari.com/article/7176520

Daneshyari.com